

Cryogenic Electron Tunneling within Mixed-Metal Hemoglobin Hybrids: Protein Glassing and Electron-Transfer Energetics

Lisa A. Dick, Isabelle Malfant, Debasish Kuila, Shannon Nebolsky, Judith M. Nocek, Brian M. Hoffman,* and Mark A. Ratner*

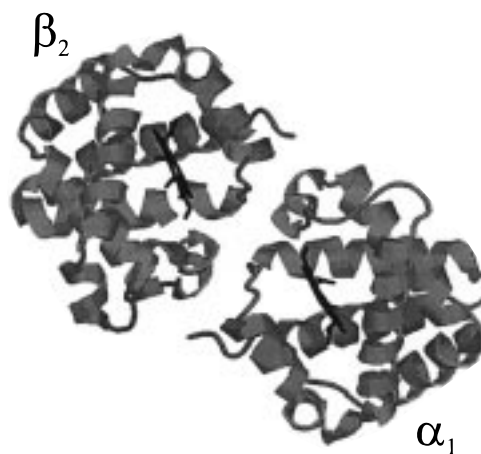
Contribution from the Department of Chemistry, Northwestern University, Evanston, Illinois 60208

Received June 9, 1998

Abstract: We report that when mixed-metal, [M, Fe] hemoglobin (Hb) hybrids, with Fe in one type of subunit and M = Zn or Mg in the other type, are embedded in clear poly(vinyl alcohol) (PVA) films, they exhibit *inter*-subunit electron transfer (ET) electron–nuclear tunneling down to cryogenic temperatures (5 K), making them the first protein system other than photosynthetic systems to exhibit such behavior. The rate constant for the (Fe²⁺Porphyrin) → (MPorphyrin)⁺ *inter*-subunit ET reaction shows a roughly temperature-invariant, quantum-tunneling regime from cryogenic temperatures (5 K) up to ca. 200 K. Some of the hybrids (depending on M and the Fe ligand) begin to show a strong increase in this ET rate constant at higher temperatures. This behavior is discussed here in terms of a recent heuristic description of ET in a glassy environment that accounts for the fact that slow solvent relaxation at low temperatures, and in particular upon cooling through a glassing transition, causes the reaction pathway to deviate from the path through the equilibrium transition state, and leads to the formation of nonequilibrium ET product states represented by points on the product surface other than that of the equilibrium product state. The analysis suggests that in regard to the dynamical modes of motion that control ET, the protein “medium” acts substantially like a frozen glass, even at room temperature. It further suggests that, although the protein acts largely as its own heat bath, the thermal characteristics of that heat bath can be modified by the external environment.

Long-range electron transfer (ET)¹ is an issue of intense interest in both synthetic and biological systems.² Mixed-metal [M, Fe] hemoglobin (Hb) hybrids, with Fe in one type of subunit and M = Zn or Mg in the other type, provide an ideal system with which to study electron transfer between redox partners rigidly held within protein partners at a fixed and crystallographically known distance and orientation.^{3–5} Flash photoexcitation of a [MP, Fe³⁺(L)P] hybrid initiates a cycle of ET between FeP and MP as shown in Scheme 1. The photoexcited MP undergoes intersystem crossing to a reactive triplet state, ³MP, which can decay, with rate constant *k*_d, or can undergo ³MP → Fe³⁺P electron transfer, with rate constant *k*_t, to produce the charge-separated intermediate, **I**, which in turn undergoes Fe²⁺P → (MP)⁺ electron transfer, rate constant *k*_b, to regenerate the ground state. Functional and structural studies showed that the mixed-metal valency hybrids, [M, Fe^{III}-L] adopt the T

quaternary structure, and that the distances and geometric relation of the heme groups *and* of the *intersubunit* interface involved in electron transfer are preserved in the metal-substituted species. Because the α₁-β₁, metal–metal distance is too great to support ET at significant rates, the [(α(FeP))₂, (β(MP))₂] tetramers studied here, as well as the complementary [(α(MP))₂, (β(FeP))₂] tetramers, thus can be treated as two independent [α₁, β₂] protein–protein electron transfer complexes where the metalloporphyrins undergoing ET are roughly parallel, with a distance of 25 Å between metals and about 17 Å edge-to-edge.^{3–6}



ET within [MP, Fe³⁺(CN⁻)P] (M = Mg, Zn) hybrids in frozen EGOH cryosolvent previously was measured from

(1) Abbreviations: ET = electron transfer; MP = metalloporphyrin; Hb = hemoglobin; EGOH = ethylene glycol.

(2) (a) de Vault, D. *Quantum-Mechanical Tunnelling in Biological Systems*, 2nd ed.; Cambridge University Press: Cambridge, 1984. (b) Marcus, R. A.; Sutin, N. *Biochim. Biophys. Acta* **1985**, *811*, 265. (c) Newton, M. D.; Sutin, N. *Annu. Rev. Phys. Chem.* **1984**, *35*, 437–480.

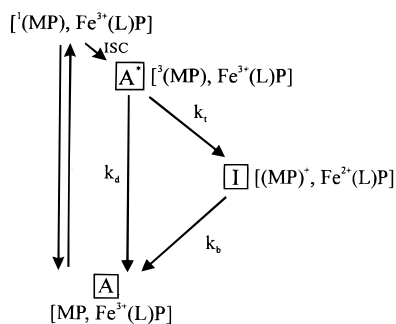
(3) (a) Natan, M. J.; Hoffman, B. M. *J. Am. Chem. Soc.* **1989**, *111*, 6468–6470. (b) McGourty, J. L.; Peterson-Kennedy, S. E.; Ruo, W. Y.; Hoffman, B. M. *Biochemistry* **1987**, *26*, 8302–8312. (c) Peterson-Kennedy, S. E.; McGourty, J. L.; Kalweit, J. A.; Hoffman, B. M. *Am. Chem. Soc.* **1986**, *108*, 1739–1746. (d) Hoffman, B. M.; Natan, M. J.; Nocek, J. M.; Wallin, S. A. *Struct. Bond.* **1991**, *75*, 85–108. (e) Natan, M. J.; Baxter, W. W.; Kuila, D.; Gingrich, D. J.; Martin, G. S.; Hoffman, B. M. *Electron Transfer in Inorganic, Organic, and Biological Systems*; Bolton, J. R., Mataga, N., McLendon, G., Eds.; *Adv. Chem. Ser.* **1991**, *228*, 201–213.

(4) Kuila, D.; Natan, M. J.; Rogers, N. P.; Gingrich, D. J.; Baxter, W. W.; Amone, A.; Hoffman, B. M. *J. Am. Chem. Soc.* **1991**, *113*, 6520–6526.

(5) Arnone, A.; Rogers, P.; Blough, N. V.; McGourty, J. L.; Hoffman, B. M. *J. Mol. Biol.* **1986**, *188*, 693–706.

(6) Kuila, D.; Baxter, W. W.; Natan, M. J.; Hoffman, B. M. *J. Phys. Chem.* **1991**, *95*, 1–3.

Scheme 1



ambient to 100 K.⁶ At temperatures less than 160 K, ET rate constants could not be determined by triplet state quenching of ³(MP) because the quenching rate is low and other forms of quenching, such as energy transfer, cannot be ignored. In the case of M = Zn, k_b varied from $k_b^{\text{Zn}}(\text{CN}^-) = 250 \text{ s}^{-1}$ at 280 K to $k_b = 80 \text{ s}^{-1}$ for $T < 160 \text{ K}$; for M = Mg, $k_b^{\text{Mg}}(\text{CN}^-) = 100 \text{ s}^{-1}$ at room temperature and fell to $k_b = 60 \text{ s}^{-1}$ at $T < 170 \text{ K}$. Analogous behavior recently has been seen for ET within a ruthenated azurin.⁷

Initial attempts to extend the hybrid measurements to lower temperatures were frustrated by the instability of cryosolvent glasses. This problem has been overcome by embedding the hybrids in clear poly(vinyl alcohol) (PVA) films,⁸ and we now report the [FeP₂, MP₂] tetramers exhibit intersubunit ET tunneling down to 5 K, making them the first protein system other than photosynthetic systems to exhibit such behavior. The rate constant for the $\text{Fe}^{2+}\text{P} \rightarrow (\text{MP})^+$ intersubunit ET reaction shows a roughly temperature-invariant, quantum tunneling regime at cryogenic temperatures, then begins to show a strong increase at temperatures above 200 K. This behavior is discussed here in terms of a recent heuristic description of ET in a glassy environment,⁹ which suggests that in regard to the dynamical modes of motion that control ET, the protein “medium” acts substantially like a frozen glass, even at room temperature.

Experimental Section

Materials. Hemoglobin was acquired from Evanston Hospital (Evanston, IL) and Life Source (Skokie, IL). $\text{K}_3\text{Fe}(\text{CN})_6$, $\text{Na}_2\text{S}_2\text{O}_4$, poly(vinyl alcohol), and 1-methylimidazole (1-MeIm) were obtained from Aldrich. Sephadex G25-150, Bis-Tris, dithiothreitol, and phytic acid (IHP) were obtained from Sigma. K_2HPO_4 and KH_2PO_4 were from Mallinckrodt. Zinc protoporphyrin and magnesium protoporphyrin were obtained from Porphyrin Products. H_2O was purified by a MilliQ water purification system (Millipore). Prepurified $\text{N}_2(\text{g})$ from Matheson was used for all deoxygenating operations and prepurified $\text{CO}(\text{g})$ from Matheson was used for CO recombination studies.

Sample Preparation. Purification of hemoglobin and preparation of the mixed-metal hybrids with an MP, M = Zn or Mg, in the one type of chain and a carboxy-ferrohememe in the other type of chain, denoted here simply as [MP; $\text{Fe}^{2+}(\text{CO})\text{P}$], has been described previously.^{4,3b} The hybrids discussed here had Zn in the β -chains, but Mg in the α -chains. All manipulations involving Zn- or Mg-substituted hemoglobins were done in the dark. Oxidation of [MP, $\text{Fe}^{2+}(\text{CO})\text{P}$] to [MP, $\text{Fe}^{3+}(\text{H}_2\text{O})\text{P}$] was done with an approximate 5-fold excess of $\text{K}_3\text{Fe}(\text{CN})_6$ at 4 °C with a $\text{N}_2(\text{g})$ stream over the solution. Excess oxidizing agent was removed by passage over G-25 resin. Samples

for measurements in ethylene glycol/buffer glass employed 50% of the cosolvent. For films, 300 mg of poly(vinyl alcohol) (PVA), 9000–10000 MW, was dissolved in 0.6 mL of 30 mM Bis-Tris/HCl pH 7.0 and heated to 80 °C for 45 min. To the cooled polymer a 0.3–0.4 mM solution of hybrid in 30 mM Bis-Tris/HCl pH 7.0 containing 1.25 equiv of IHP (per monomer of hemoglobin) was added in a total volume of 200 μL or less. The polymer volume was about 10 times that of the protein. The protein/PVA mixture was dropped onto 1 cm \times 2 cm quartz slides and allowed to dry at 4 °C, resulting in films which were about 15% H_2O by gravimetric analysis and approximately 0.5 μm thick. For samples with a ligand other than H_2O , the buffers were the same as above but with 10 mM KCN or 200 mM 1-MeIm. Measurements of CO rebinding to [MgP; $\text{Fe}(\text{CO})\text{P}$] hybrids after photolysis confirm that the photolyzed hybrids under PVA film conditions are fully in the tetrameric T state.¹⁰

The short path length PVA samples for low-temperature optical studies are very concentrated, but the possibility of inter-hemoglobin interactions was ruled out by the observation that the addition of excess bovine serum albumin (5-fold), a non-ET active protein for dilution, as well as dithiothreitol, had no effect on the measurements.

Instrumentation. Optical spectra were recorded by an HP 8451A diode array spectrophotometer. A Waters 650 HPLC was used for protein purification. To confirm purity, isoelectric focusing of HPLC fractions was done with a Pharmacia Phast System.

The actinic source for flash photolysis was the frequency-doubled 532 nm line of a Quantel YG-660 or Continuum Surelite I YAG laser (30 mJ, $t \sim 7 \text{ ns}$). Conventional analyzing optics and data collection were employed. Typically, 25 transients were averaged for triplet decays and 200 transients for intermediate signals in the ET intermediate. A locally built optical dewar (W. H. Sales, Ltd.) was used for experiments down to $T = 77 \text{ K}$. For helium experiments, an Oxford CF 1204 cryostat, transfer line, and ITC4 temperature controller were employed.

Kinetics. Photoexcitation of [MP, FeP] hybrids generates a long-lived ³(MP) triplet state, **A*** (Scheme 1), a powerful reducing agent that leads to the production of the charge-separated intermediate, **I**. The time course of species **A***, as shown in Scheme 1, is

$$\mathbf{A}^*(t) = \mathbf{A}^*(0)e^{-(k_d+k_i)t} = \mathbf{A}^*(0)e^{-k_p t} \quad (1)$$

and that of the intermediate, **I**, is

$$I(t) = k_i \mathbf{A}^*(0) \left\{ \frac{e^{-k_p t} - e^{-k_b t}}{k_b - k_p} \right\} \quad (2)$$

where $\mathbf{A}^*(0)$ is the initial concentration of the reactive triplet species, k_p is the sum of the intrinsic triplet decay, k_d , and the photoinitiated electron-transfer rate constant, k_i , and the rate constant for return of **I** to the ground state is k_b . The Marquardt nonlinear least-squares algorithm was used to fit the data.¹¹

Results

Optical Spectra of Hybrids in Films. The room-temperature optical spectra of the [βMP ; $\alpha\text{Fe}^{3+}(\text{L})\text{P}$] hemoglobin hybrids embedded in PVA films are identical to those previously observed in aqueous solution or cryosolvent.^{3c} In all cases, upon cooling hybrids in the PVA film, the optical spectra sharpen smoothly without discontinuity, implying that the heme retains its original ligation state during the cooling process. For L = H_2O , this result contrasts with the previous findings that the [βZnP ; $\alpha\text{Fe}^{3+}(\text{H}_2\text{O})\text{P}$] hybrid frozen in an aqueous ethylene glycol cryosolvent glass undergoes a ligation state change upon cooling below $\sim 250 \text{ K}$.^{3c}

Triplet-State Measurements. The triplet decays for the [MP, Fe^{2+}P] and [MP, $\text{Fe}^{3+}(\text{L})\text{P}$] hybrids in PVA films have been measured down to 5 K. The intrinsic ³(MP) decay curves, M = Mg or Zn, for $\text{Fe}^{2+}(\text{P})$ hybrids, which cannot show ET,

(7) Skov, L. K.; Pascher, T.; Winkler, J. R.; Gray, H. B. *J. Am. Chem. Soc.* **1998**, *120*, 1102.

(8) Schenck, C. C.; Parson, W. W.; Holten, D.; Windsor, M. W. *Biophys. J.* **1981**, *36*, 479–489.

(9) (a) Klosek-Degas, M. M.; Hoffman, B. M.; Matkowsky, B. J.; Nitzan, A.; Ratner, M. A.; Schuss, Z. *J. Chem. Phys.* **1989**, *90*, 1141–1148. (b) Hoffman, B. M.; Ratner, M. A. *Inorg. Chim. Acta* **1996**, *243*, 233–238; for related work see references therein.

(10) Dick, L. Ph.D. Thesis, Northwestern University, 1997.

(11) Bevington, P. *Data Reduction and Error Analysis for the Physical Sciences*; McGraw-Hill Book Company: New York, 1969.

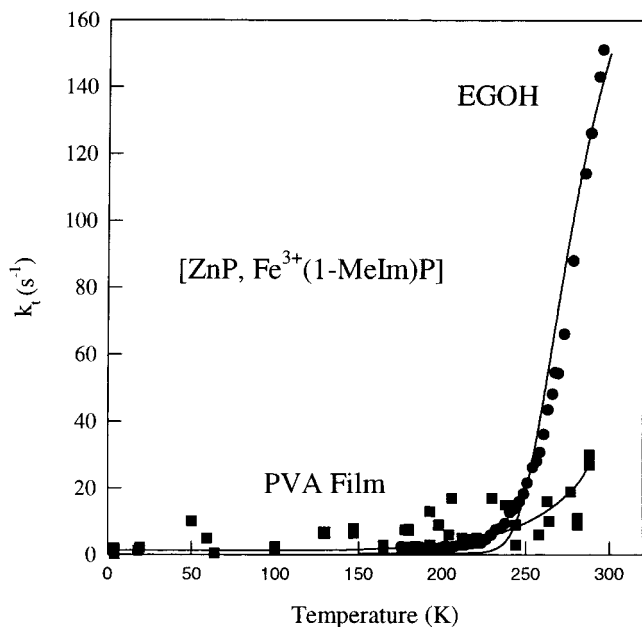


Figure 1. Triplet decay rate constants versus temperature for the [ZnP, Fe³⁺(1-MeIm)P] hybrid in EGOH cryosolvent (filled circles) and in PVA glass (filled squares), along with modeling descriptions of the data according to eqs 4 and 5. The parameters employed here are shown in Table 1.

are exponential at all temperatures in the films, as in cryosolvents.^{6,3c} The decay rate constants, k_d , are very weakly temperature dependent, with $k_d \sim 10\text{--}20\text{ s}^{-1}$ for $M = \text{Mg}$ and $k_d = 30\text{--}40\text{ s}^{-1}$ for $M = \text{Zn}$.

Electron-transfer quenching by the ferriheme in an [MP, Fe³⁺(L)P] hybrid enhances the ³(MP) decay, whose observed rate constant becomes $k_p = k_d + k_t$, where k_t is the ET rate constant. The triplet progress curves for the [ZnP; Fe³⁺(L)P] hybrids also are exponential, and Figure 1 presents the temperature dependence of k_t for the [ZnP; Fe³⁺(1-MeIm)P] hybrid in PVA, along with data for this hybrid in EGOH cryosolvent for a range of temperatures, 170 K < T < 300 K. There is measurable ET quenching for the hybrid in PVA for temperatures above perhaps 250 K, although much less than in EGOH, where strong ET quenching appears above ~ 200 K. However, for the PVA films at lower temperatures the decay rate constants for oxidized and reduced hybrids in PVA do not differ significantly, and the same is true for $L = \text{H}_2\text{O}$ and CN^- , as well. When traces from all three [ZnP; Fe³⁺(L)P] hybrids at 5 K are overlaid (data not shown), slight differences in their lifetimes can be observed, with the rate of disappearance following the order $L = \text{H}_2\text{O} > \text{CN}^- > 1\text{-MeIm}$. However, overall, these data give no compelling evidence for cryogenic ET, as was the case in the study of ruthenated Zn-substituted cytochrome *c* by Maki and co-workers.¹²

The triplet decays for [MgP, Fe³⁺(L)P] hybrids in EGOH also are exponential,⁶ with ET quenching observable at temperatures > 250 K. However, the decays in the PVA films are biphasic. Over the range 5–300 K, the more rapid phase contributes a temperature-invariant fraction, $\sim 40\%$, and decay constant $k_p = 50\text{ s}^{-1}$. For [MgP, Fe³⁺(CN⁻)P], the slower decay constant decreases slightly with cooling, from 20 s⁻¹ at 300 K to 12 s⁻¹ at 200 K, then remains invariant to 5 K. For [MgP, Fe³⁺(1-MeIm)P], the slower decay rate constant, k_{p1} , is essentially temperature invariant at $\sim 12\text{ s}^{-1}$. As with the Zn

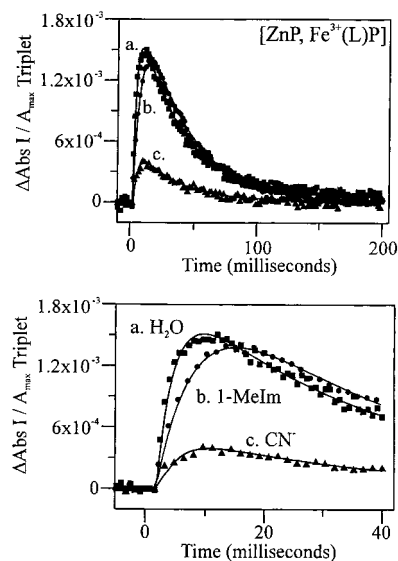


Figure 2. Kinetic progress curves for the charge separated intermediate, **I**, for [Fe³⁺(L)P, ZnP] hybrids embedded in PVA film at 5 K. Symbols are experimental data points, solid lines are the fits to eq 2: (a) $L = \text{H}_2\text{O}$, (b) $L = 1\text{-MeIm}$, and (c) $L = \text{CN}^-$. Each trace is the average of approximately 250 shots. Upper: Full time course. Lower: Expansion of short time data.

hybrids, at 5 K there are only small differences in rate constants among differently ligated Mg hybrids. Hence, once again triplet-decay data do not give evidence for electron-transfer quenching at liquid helium temperatures.

Charge-Separated Electron-Transfer Intermediate. (a) ET at $T = 5$ K. Although photoinitiated ET at cryogenic temperatures cannot be verified by triplet quenching measurements, direct monitoring of the optical absorbance spectrum of the ET intermediate, **I**, shows that the photoprocess persists down to 5 K and that we can reliably measure the rate constant for the $\text{Fe}^{2+}\text{P} \rightarrow (\text{ZnP})^+$, return ET step. Figure 2 presents representative short-time and full progress curves for **I** (Scheme 1) as detected at the 436 nm ³(ZnP)/(ZnP) isosbestic point following flash excitation of [ZnP; Fe³⁺(L)P] hybrids in PVA films at 5 K. This wavelength corresponds roughly to a maximum in the [Fe²⁺ P/Fe³⁺ P] difference spectrum, and the signal can definitively be ascribed to the ferriheme reduction to form **I** because no such signal is seen for the Fe²⁺ P hybrid, which cannot undergo ET. As additional confirmation, the expected amplitudes of the absorbance difference for **I** were calculated with eq 2 and found to be in satisfactory agreement with experiment. A fortunate feature of the Hb hybrid system for studies of cryogenic ET is that k_d is so low that even for a very small value of the ET rate constants, k_t , of $\sim 1\text{ s}^{-1}$ or less, the quantum yield for triplet-state ET, $\phi = k_t/k_p \sim k_t/(k_d + k_t)$, ignoring possible small energy-transfer contributions, is sufficiently large as to give a detectable signal from **I**.

The kinetic progress curves for **I** can be well fit to eq 2, with k_b (Scheme 1) corresponding to the rate of appearance ($k_b > k_p$). The ET rate constants at 5 K for the [ZnP; Fe³⁺(L)P] hybrids are $k_b = 335, 170,$ and 226 s^{-1} for $L = \text{H}_2\text{O}, 1\text{-MeIm},$ and CN^- ; in each case, k_p corresponds to the rate constant of the triplet decay, as required for the ET photocycle of Scheme 1. Thus, the photoinitiated ET process that produces **I** in fact persists down to 5 K, even though its rate constant is small, while the return reaction not only occurs at 5 K, but is readily characterized. The fits to the timecourses for the intermediate were not significantly improved by use of an equation that employed multiple kinetic phases nor by an attempt to use a

(12) Zang, L.-H.; Maki, A. H. *J. Am. Chem. Soc.* **1990**, *112*, 4346–4351.

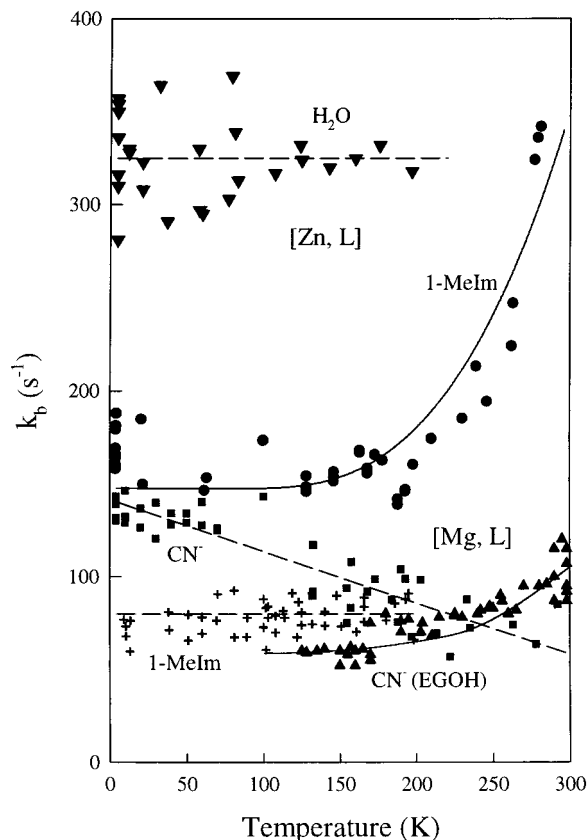


Figure 3. Temperature dependence of k_b (rate constant for the $[(MP)^+, Fe^{2+}(L)P] \rightarrow [(MP), Fe^{3+}(L)P]$ reaction). Fits with eq 3 are solid lines, and parameters are listed in Table 1; dashed lines are to guide the eye only. Down triangle: $M = Zn, L = H_2O$ in PVA. Circle: $M = Zn, L = 1-MeIm$ in PVA glass. Square: $M = Mg, L = CN^-$ in PVA glass. Plus: $M = Mg, L = 1-MeIm$ in PVA glass. Up triangle: $M = Mg, L = CN^-$ in EGOH cryosolvent.

distribution of rate constants for the back ET rate constant, k_b , or for the triplet decay, k_p . Thus any distribution in protein conformations that may occur in the film is not manifested in the observed behavior of **I**.

The $[MgP, Fe^{3+}(L)P]$ hybrids likewise show transient-absorbance signals from **I** at the $^3MgP/MgP$ isosbestic point (data not shown) which are well fit by a single kinetic phase, eq 2. For the $[MgP, Fe^{3+}(CN^-)P]$ and $[MgP, Fe^{3+}(1-MeIm)P]$ hybrids at 5 K the fits yield $k_b = 150$ and $76 s^{-1}$, respectively, with values of $k_p = 12 s^{-1}$ that correspond to the rate constant for the major component of the triplet decay, k_{p1} ; thus the hybrids that contribute to the major decay component exhibit ET, but those of the minor component do not. We were concerned that the progress curve for the ET intermediate in these Mg hybrids might be distorted by an unassigned transient signal detected in films containing MgHb; and indeed a Mg transient signal of about 20% of an ET intermediate signal height was observed for $[MgP, Fe^{2+}P]$ hybrids. However, the signals from the ET intermediate in the $[MgP, Fe^{3+}(L)P]$ samples at 5 K cannot be seriously distorted because they can be well described by a single kinetic phase where the ET rate constant is significantly different for different ligands.

(b) Variable-Temperature ET. We have measured the temperature dependences of k_b for $[MP; Fe^{3+}(L)P]$ hybrids, $M = Zn$ and Mg , in PVA films at temperatures of 5 K and above, and they are plotted in Figure 3, along with data for hybrids in EGOH, for $T > 170$ K. The ET intermediate produced by photolysis of the $[ZnP; Fe^{3+}(1-MeIm)P]$ hybrid in PVA could

be examined over the complete temperature range, 5–300 K. The cryogenic rate constant, $k_b \sim 170(15) s^{-1}$, remains temperature invariant (or perhaps falls slightly) between 5 and 200 K, then increases to $\sim 330 s^{-1}$ at ~ 290 K. For the $M = Zn, L = H_2O$ hybrid in PVA, $k_b = 335(25) s^{-1}$ at 5 K, a roughly 2-fold greater value than for $L = 1-MeIm$, and k_b again is temperature invariant between 5 and 200 K; in this case we did not collect data at higher temperatures because the ET process became partially irreversible and optical spectra show an accumulation of $Fe^{2+}P$. For the $[ZnP; Fe^{3+}(CN^-)P]$ hybrid, signals for **I** were weak and difficult to follow; we do not discuss them further.

For the $[MgP; Fe^{3+}(1-MeIm)P]$ hybrid in PVA, $k_b \sim 75 s^{-1}$ at 5 K and remains temperature invariant at $k_b \sim 100 s^{-1}$ over the temperature range measured, 5–200 K (Figure 3); for $[MgP, Fe^{3+}(CN^-)P]$ hybrids, $k_b \sim 140 s^{-1}$ at 5 K and actually *decreases* ~ 2 -fold by ambient temperature. This same “negative activation energy” feature has been observed for several reactions of the photosynthetic RC.¹³ For the same $L = CN^-$ hybrid in EGOH, k_b increases gently from $k_b \sim 50 s^{-1}$ at ~ 150 K to $\sim 100 s^{-1}$ at ~ 300 K.⁶

Theoretical Modeling. The full temperature variation of the intersubunit ET rate constants can be described by a phenomenological model that describes electron-transfer reactions in slowly relaxing media, such as glassy solvents and proteins that undergo glassing transitions.⁹ The model recognizes that it is necessary to treat the ET process as taking place not on a one-dimensional configuration-coordinate potential surface, as in the usual idealization, but on a 2-D potential surface where one dimension subsumes the inner-sphere coordinates and the other the outer-sphere ones. For an equilibrium ET reaction on such a surface, with driving force ΔG° , the steepest-descent, equilibrium reaction path is described by the total equilibrium reorganization energy, $\lambda_s = \lambda_o + \lambda_i$, where λ_o and λ_i are the equilibrium outer- and inner-sphere contributions. However, as discussed in detail,⁹ when outer-sphere relaxation is *not* rapid, the slow solvent relaxation causes the reaction pathway to deviate from the path through the equilibrium transition state. *Our premise^{9b}* is that the slowing down of solvent motions causes the formation of product in nonequilibrium states that are represented by points on the product surface other than that of the equilibrium product state, and that as a result the formation of the nonequilibrium ET product states is on average describable by taking the driving force and reorganization energy as undergoing correlated changes with temperature such that their sum remains temperature independent, $\Delta G(T) + \lambda(T) = \Delta G^\circ + \lambda_s$ (this sum is the vertical distance (in energy) between the reactant and product surfaces at the equilibrium reactant configuration). The physical model, which is described further in the Discussion below, was realized mathematically through use of the two-mode expression of Hopfield.¹⁴ Within the model only the temperature-dependent effective reorganization energy appears explicitly, $\lambda(T)$, with a temperature-independent inner-sphere term, λ_i , and temperature-dependent outer-sphere term, $\lambda_o(T)$. The resulting ET rate constant is given as:

$$k = \left(\frac{\pi^{1/2} V^2}{\hbar} \right) \left(\frac{1}{B_H} \right)^{1/2} \exp \left\{ \frac{-(\Delta G^\circ + \lambda_s)^2}{4B_H} \right\} \quad (3)$$

where

(13) Shopes, R. J.; Wraight, C. A. *Biochim. Biophys. Acta* **1990**, *1020*, 239–246. Harywich, G.; Beiser, G.; Langenbacher, P.; Müller, P.; Richter, A.; Ogrodnik, A.; Scheer, H.; Michel-Beyerle, M. B. *Biophys. J.* **1997**, *A8*, 71.

(14) Hopfield, J. J. *Proc. Natl. Acad. Sci. U.S.A.* **1974**, *71*, 3640–3644.

$$B_H = k_B T_c^{(o)} \lambda_o(T) \coth\left(\frac{2T_c^{(o)}}{T}\right) + k_B T_c^{(i)} \lambda_i \coth\left(\frac{2T_c^{(i)}}{T}\right) \quad (4)$$

$$\lambda(T) = \lambda_i + \lambda_o(T) = \lambda_i + f(T)\lambda_o \quad (5a)$$

$$f(T) = \begin{cases} \exp\{-B/(T - T_g)\} & T > T_g \\ 0 & T < T_g \end{cases} \quad (5b)$$

The temperature-dependent function, $f(T)$, chosen to describe the unglassing of the medium is commonly used for glass formers; T_g is an equilibrium glass transition temperature below which all solvent motion is quenched; B is a pseudoactivation energy for solvent motion at temperatures $T > T_g$. With this function, $\lambda(T) = \lambda_i$ when $T < T_g$ and $\lambda(T) \rightarrow \lambda_s$ when $T \gg T_g$. Finally, $T_c(\alpha) = h\nu_\alpha/k_B$, where ν_o and ν_i are the outer- and inner-sphere-mode vibration frequencies.¹⁵ We ignore possible temperature variations in the ET matrix element, V^2 , as being of secondary impact, although they may well be responsible for such interesting phenomena as the ~ 2 -fold decrease in k_b for [MgP, Fe³⁺(CN⁻)P] hybrids from 5 K to ambient.

This modeling routine was used to describe the temperature dependence of the ET rate constants for the mixed-metal hemoglobin hybrids in ethylene glycol cryosolvent (EGOH) and PVA film, as previously described.^{9b} ΔG° values were determined previously by Hawkrige et al. by direct electrochemical methods.¹⁶ A limit was placed on the sum of $-\Delta G^\circ$ values for the forward and back reactions based on the phosphorescence energy maxima (1.72 and 1.70 V for ³ZnHb and ³MgHb, respectively). In fitting the data, the initial estimates for the total reorganization energy were $\lambda_s \sim 1$ eV,¹⁷ then adjusted; the partition between inner- and outer-sphere contributions also was used as a fit parameter. The vibrational constants, $T_c^{(o)}$ and $T_c^{(i)}$, were fixed at 20 and 400 K as representing typical values for outer- and inner-sphere vibrational modes. The glassing temperature of an EGOH cryosolvent was given its reported value of 200 K;¹⁸ the glassing temperature of solid PVA is known from differential scanning calorimetry to be near 280 K.¹⁹ The parameter B , the pseudoactivation energy for unglassing, was held constant at a typical value of 150 K. Modeling was performed for those cases where the data included a regime where the rate constant increases with T ; hybrids whose rates could not be measured at a high enough temperature to achieve this behavior are not discussed.

Figure 1 presents a model simulation of the temperature dependences of k_i for the [ZnP, Fe(1-MeIm)P] hybrid in EGOH cryosolvent ($T > 175$ K) and in PVA glass, while Figure 3 presents the model calculation of k_b for this hybrid in PVA ($5 < T < 300$ K). Considering the hybrid in PVA film, the temperature dependences of both k_i and k_b are well described by the same reorganization-energy parameter set, including glassing parameters, and vibrational frequencies (Table 1). This includes a reasonable total reorganization energy ($\lambda \sim 1$ V),

(15) The separation of high-frequency, local vibrational contributions (T-independent) and diffusive, relaxing contributions (T-dependent) has been used to model T-dependent Stokes shift data on chromophores intercalated in DNA (Brauns, E. B.; Murphy, C. J.; Berg, M. A. *J. Am. Chem. Soc.* **1998**, *120*, 2449). In that case, as in this, the T-dependent part, though best understood as local solvation, was "slaved" to the solvent glassing.

(16) King, B. C.; Hawkrige, F. M.; Hoffman, B. M. *J. Am. Chem. Soc.* **1992**, *114*, 10603–10608.

(17) Meade, T. J.; Gray, H. B.; Winkler, J. R. *J. Am. Chem. Soc.* **1989**, *111*, 3–4356.

(18) Fink, A. L.; Greeves, M. A. *Methods Enzymol.* **1979**, *63*, 336–371.

(19) Iben, I. E. T.; Braunstein, D.; Doster, W.; Frauenfelder, H.; Hong, M. K.; Johnson, J. B.; Luck, S.; Ormos, P.; Schulte, A.; Steinbach, P. J.; Xie, A. H.; Young, R. D. *Phys. Rev. Lett.* **1989**, *62*, 1916–1919.

Table 1. Parametrization of k_i and k_b ET Rate Constants for Mixed-Metal Hb Hybrids in EGOH Cryosolvent and PVA Film, according to eq 3^a

hybrid	medium	T_g^a (K)	rate constant	$-\Delta G^\circ^b$ (V)	λ_s^a (V)	outer sphere (fraction λ_s)
ZnFe(1-MeIm)	EGOH	200	k_i	0.78	1.00	0.95
	PVA film	270	k_i	0.78	1.15	0.95
	PVA film	270	k_b	0.94	1.15	0.95
MgFe(CN ⁻)	EGOH ^d	200	k_i	0.51 ^c	0.95	0.78
	EGOH ^d	200	k_b	1.19 ^c	0.95	0.78

^a Substitutions: Zn in β -chains; Mg in α -chains. T_g is fixed for each medium as discussed in the text. $\lambda_s = \lambda_o + \lambda_i$. Other fixed parameters were the following: $T_c^{(o)} = 20$ K, $T_c^{(i)} = 400$ K, and $B = 150$ K. The tunneling matrix element, V , in eq 3 was used as a scaling parameter; it varied minimally, between 7.5×10^{-8} and 2.4×10^{-6} eV. ^b The sum of $-\Delta G^\circ$ for k_b and k_i was constrained to equal the phosphorescence energy maximum for each MHB. ^c Based on values obtained from King et al.: *J. Am. Chem. Soc.* **1992**, *114*, 10603–10608. ^d Data from ref 6.

only a small fraction of which is inner sphere. Considering the data for k_i in the two media, the same reorganization parameter set describes the data for this hybrid in EGOH and PVA film, with the sole exception of a higher glassing temperature for the film (270 K) than for the cryosolvent (200 K). We take this internal consistency to be a strong support for the model.

The previously measured^{6,10} rate constants, k_b (Figure 3) and k_i , for the [MgP, Fe³⁺(CN⁻)P] hybrid in EGOH cryosolvent ($T > 100$ K) likewise can be well described by a one-parameter set, along with the proper exoergicity. That set includes the same glassing parameters as used for the Zn hybrid and the same overall reorganization energy; only the partition between outer- and inner-sphere contributions is somewhat different (Table 1). The difference between λ_i for the [MgP, Fe³⁺(CN⁻)P] and [ZnP; Fe(1MeIm)P] hybrids perhaps is related to the different behaviors seen earlier for anionic and neutral ligands.³

For the [MgP, Fe³⁺(CN⁻)P] hybrid in PVA film k_b decreases with temperature between 5 and ~ 300 K. (Figure 3). Although such data cannot be fit meaningfully with the model, we take this to reflect the fact that T_g is higher for PVA and the system is in the inverted regime with only λ_i contributing, and $|\Delta G^\circ/\lambda_i| > 1$. In this regime, quantum modeling²⁰ indeed yields a weak rate constant decrease with increasing temperature, essentially for Franck–Condon reasons.

Discussion

Intersubunit ET within mixed-metal [β MP; α Fe³⁺(L)P] hemoglobins embedded in PVA films has been studied down to 5 K. The appearance of the charge-transfer intermediate **I** down to $T = 5$ K confirms that photoinitiated intersubunit, ³(MP) \rightarrow Fe³⁺(L)P ET persists to cryogenic temperature, even though its rate constant, k_i , is too low to be measured reliably. The rate constant, k_b , for the return reaction, Fe²⁺(L)P \rightarrow (MP)⁺, is readily measured down to 5 K by monitoring the timecourse of **I**. For all the hybrids, the rate constant k_b shows quantum-tunneling temperature independence (or a small decrease in rate constant with increasing temperature) from 5 K to at least ~ 200 K. Such behavior is well-known in the photosynthetic reaction center,²¹ but no other protein-based system has displayed this

(20) Bixon, M.; Jortner, J. *Adv. Chem. Phys.* In press. Bixon, M.; Jortner, J. *J. Phys. Chem.* **1991**, *95*, 1941–1949. Todd, M. D.; Nitzan, A.; Ratner, M. A.; Hupp, J. T. *J. Photochem. Photobiol.* **1994**, *82*, 87.

(21) (a) Shopes, R. J.; Wraight, C. A. *Biochim. Biophys. Acta* **1987**, *893*, 409–425. (b) McDowell, L. M.; Kirmaier, C.; Holten, D. *J. Phys. Chem.* **1991**, *95*, 9379–9389.

behavior, and for most small-molecule model systems, measurements cannot be conducted to cryogenic temperatures because ET precipitously shuts off at the glassing temperature of the solvent. Thus, Wasielewski and co-workers attained electron transfer at 5 K with a carefully designed porphyrin based donor acceptor system,²² although the decay rates were substantially slower at 5 K ($t = 520$ ps) than at room temperature ($t = 2.9$ ps).

There are several views of such quantum-tunneling behavior. First, if the reorganization energy were equal to $-\Delta G^\circ$ (the so-called optimal regime), all ET theories predict very weak T dependence, though the rate would increase with a drop in T . Second, ET can be temperature independent over a larger free energy range if it is coupled dominantly to vibrations whose vibrational quantum exceeds the thermal energy available. Quantum dynamical studies of the usual harmonic model for ET indeed show a very weak increase in k for a decrease in temperature, due to enhanced tunneling in the inverted regime.²⁰ Third, a spin-glass coupling model suggests "false tunneling", T -dependent behavior.²³ Recently a fourth option was suggested based on a study of thermodynamics in *R. sphaeroides* RC's which concluded that the lack of temperature dependence was a result of adiabatic ET near the strong coupling limit rather than nonadiabatic ET coupled to vibrations.²⁴ This model, like the optimal regime, has a very small activation barrier where reactant and product potential surfaces cross near the bottom of the reactant surface.

Several groups have observed an essentially activationless behavior in the inverted region with model compounds. Liang *et al.* have shown that intramolecular ET in the inverted region is activationless, for Decalin-bridged donor/acceptor molecules.²⁵ Kroon *et al.* studied a wide range of driving forces from normal to inverted between closely related bridged donor/acceptor organic molecules.²⁶ Classical Marcus theory adequately described temperature dependencies in the normal region but did not describe the observed temperature independence in the inverted region (vibronic models can achieve this T independence).²⁷ Chen *et al.*²⁸ observed a weak T dependence and attributed it to solvent reorganization energy.

When the $M = \text{Mg}$, $L = \text{CN}^-$ and $M = \text{Zn}$, $L = 1\text{-MeIm}$ hybrids are warmed above the quantum-tunneling regime (temperatures above ~ 200 K), k_b shows a strong but not abrupt increase with increasing T , overall behavior that recalls the very earliest studies of low-temperature ET on the photosynthetic reaction center by DeVault and Chance.^{2a} We have described the full temperature variation of this type, focusing on the hybrids, through a heuristic model of the electron-transfer reaction in glassy solvents and in proteins which undergo glassing transitions.⁹ This model recognizes that one must specifically take into account the outer-sphere relaxation of the

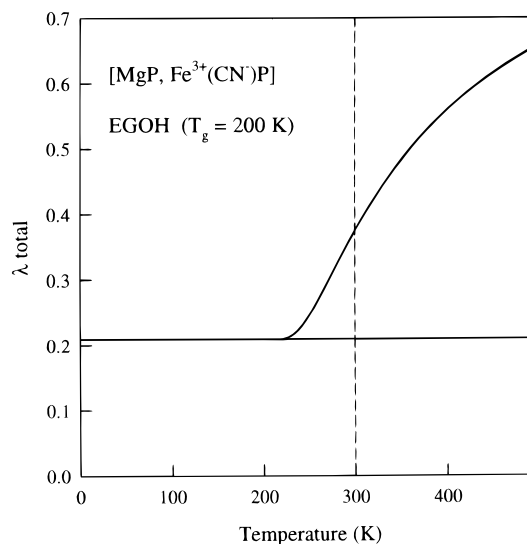


Figure 4. Temperature dependence of the effective reorganization energy, $\lambda(T)$ (eV), for the [MgP, Fe(CN)⁻P] hybrid according to eq 5a. The dashed vertical line at 300 K indicates the upper limit of our experimental data collection. Parameters used: $\lambda_i = 0.21$, $\lambda_o = 0.74$ eV, and thus $\lambda_s = 0.95$ eV (Table 1).

"medium" that surrounds the redox centers. In slowly relaxing media, the system trajectories *cannot* proceed through the normal transition state: slow solvent relaxation causes the reaction pathway to vary substantially from the equilibrium reaction path, resulting in increased effective barriers and reduced effective outer-sphere reorganization energies compared to the path through the equilibrium transition state. This phenomenon is modeled^{9b} by treating the ET process as taking place not on a one-dimensional configuration-coordinate potential surface, as in the usual idealization, but on a 2-D potential surface where one dimension subsumes the inner-sphere coordinates and the other the outer-sphere ones. It is assumed that the slowing down of medium motions at low temperatures, and in particular upon cooling through a glassing transition, leads to the formation of nonequilibrium ET product states represented by points on the product surface other than that of the equilibrium product state, and that as a result the ET reaction is on average describable by taking the driving force and reorganization energy as undergoing correlated changes with temperature such that their sum remains temperature independent. According to this assumption, it is *not* proper to take just one or the other as changing.²² As a consequence, in the mathematical realization of the model through use of the two-mode expression of Hopfield,¹⁴ the expression for the ET rate constant, eqs 1–5, explicitly exhibits only the temperature-dependent effective reorganization energy, $\lambda(T)$, with a temperature-independent inner-sphere term and temperature-dependent outer-sphere term, eq 5a. Figure 4 shows the temperature dependence of the effective reorganization energy, $\lambda(T)$, for the [MgP, Fe(CN)⁻P] hybrid in EGOH, calculated by using the functional form of eq 5a for $\lambda(T)$ and the fit parameters of Table 1.

Below the glassing temperature of the medium, only the inner-sphere reorganization contributes. At high temperatures, sufficiently far above the protein glassing temperature, both the inner-sphere and outer-sphere components contribute fully, and the outer-sphere component is much larger. However, according to the fits to the experimental data, ambient temperatures are *not* high. As shown in Figure 4, for the [MgP, Fe(CN)⁻P] in EGOH, only a relatively small amount of the outer-sphere contribution to λ is achieved by 300 K, and this is even more true in PVA, where T_g is higher. *In short, this model suggests*

(22) (a) Wasielewski, M. R.; Johnson, D. G.; Svec, W. A.; Kersey, K. M.; Minsek, D. W. *J. Am. Chem. Soc.* **1988**, *110*, 7219–7221. (b) Wasielewski, M. R.; Gaines, G. L., III; O'Neil, M. P.; Svec, W. A.; Niemczyk, M. P. *J. Am. Chem. Soc.* **1990**, *112*, 4559–4560.

(23) Dakhnovskii, Y.; Lukchenko, V.; Wolynes, P. *J. Chem. Phys.* **1996**, *104*, 1875.

(24) Woodbury, N. W.; Peloquin, J. M.; Alden, R. G.; Lin, X.; Lin, S.; Taguchi, A. K. W.; Williams, J. C.; Allen, J. P. *Biochemistry* **1994**, *33*, 8101–8112.

(25) Liang, N.; Miller, J. R.; Closs, G. L. *J. Am. Chem. Soc.* **1990**, *112*, 5353–5354. Liang, N.; Miller, J. R.; Closs, G. L. *J. Am. Chem. Soc.* **1989**, *111*, 8740–8741.

(26) Kroon, J.; Oevering, H.; Verhoeven, J. W.; Warman, J. M.; Oliver, A. M.; Paddon-Row, M. N. *J. Phys. Chem.* **1993**, *97*, 5065–5069.

(27) Barbara, P. F.; Meyer, T. J.; Ratner, M. A. *J. Phys. Chem.* **1996**, *100*, 13148. Jortner, J. *J. Chem. Phys.* **1976**, *64*, 4860.

(28) Chen, P.; Mecklenburg, S. L.; Meyer, T. J. *J. Phys. Chem.* **1993**, *97*, 13126–13131.

that the protein acts as the primary solvent “medium” of the redox centers involved, and behaves substantially as a frozen glass, even at room temperature.²⁹ Moreover, to some degree at least, it appears that the glassing temperature of the protein is coupled (“slaved”^{19,30}) to that of its environment, because T_g is different for the two media. Such a coupling of ET to protein dynamics suggests a link to the study of protein dynamics through measurements of CO recombination, where the degree to which internal protein dynamics are coupled to the protein surface is an important question.^{31,32}

How persuasive is this description? Clearly, the precise values of the parameters reported are not particularly significant in themselves. Indeed, to avoid making this an exercise in parameter fitting a number of the parameters in the description, including B and $T_c^{(i)}$, are fixed at reasonable values, and different definitions of T_g could be used²⁹ provided they preserve the difference between PVA and EGOH. Changing any of these parameters within reasonable bounds would still lead to acceptable fits, but with somewhat different fit parameters. However, by fixing these parameters we are left with *only* the inner- and outer-sphere reorganization energies as fitting variables, and we place particular weight on the fact that with this limitation, the model nonetheless gives a consistent description of the temperature response of *both* k_i and k_b for two different hybrids in two different media. In particular, this approach does *not* lead to the large, nonphysical values for the

reorganization energy which are necessary if a “one-mode” description is used in an attempt to explain the observed behavior.¹⁷

The model further makes testable predictions, through the study of hybrids embedded in trehalose glass,^{31,33} or encapsulated in sol-gels.³⁴ The glassing temperature for trehalose varies with the extent of hydration, and can be adjusted from $T_g \sim -60$ to 114 °C.³⁵ Hence, we can directly examine the degree to which ET *within* a protein complex is governed by coupling to the glassing of the external medium. Further, the parameters of Table 1 lead the model to predict that warming the hybrids to temperatures appreciably above ambient will lead to further unglassing, and that this should result in substantial further increases in the rate of intersubunit electron transfer. Denaturation makes it impossible to test this prediction for hybrids in fluid solution, but Hb encapsulated in a porous sol-gel is protected from denaturation up to temperatures near that of boiling water!³⁶ In future work we shall apply these techniques to test the interpretation of the electron-transfer measurements reported here.

Acknowledgment. We are grateful for support to the NIH (HL13531 and HL51084; B.M.H.) and to the Chemistry Division of the ONR (M.R.). We thank the late Mr. Gregory Martin for his help in the preparation of Hb hybrids. Initial work benefitted from the assistance of Mr. Andrew Everest.

JA982032G

(29) Note also, we have used for T_g in eq 5b the measured glass transition temperature, while the usual approach in describing glass-formers above T_g replaces T_g by T_o , the so-called equilibrium glass transition temperature ($T_o \cong T_g - 50$ K), e.g.: Ratner, M. A. In *Polymer Electrolyte Reviews*; MacCallum, J. R., Vincent, C., Eds.; (Elsevier: London; 1987; Vol. I, p 173). This has no impact on the important points of the current model, namely the partitioning in eq 5 and the prediction of further changes above ambient temperature.

(30) Frauenfelder, H.; Sligar, S. G.; Wolynes, P. G. *Science* **1991**, *254*, 1598–1603.

(31) Sastry, G. M.; Agmon, N. *Biochemistry* **1997**, *36*, 7097–7108.

(32) Note, in considerations of the distance dependence of the ET matrix element, V^2 , it has been proposed that a protein behaves like an organic glass. Moser, C. C.; Keske, J. M.; Warncke, K.; Farid, R. S.; Dutton, L. P. *Nature* **1992**, *355*, 796–802

(33) (a) Hagen, S. J.; Hofrichter, J.; Eaton, W. A. *J. Phys. Chem.* **1996**, *100*, 12008–12021. (b) Gottfried, D. S.; Peterson, E. S.; Sheikh, A. G.; Wang, J.; Yang, M.; Friedman, J. M. *J. Phys. Chem.* **1996**, *100*, 12034–12042

(34) Ellerby, L.; Clinton, N. R.; Nishida, F.; Yamanaka, S. A.; Dunn, B.; Valentine, J. S.; Zink, J. I. *Science* **1992**, *225*, 1113–1115. Zink, J.; Valentine, J. S.; Dunn, B. *New J. Chem.* **1994**, *18*, 1109–1115. Dave, B. C.; Dunn, B.; Valentine, J. S.; Zink, J. I. *Anal. Chem.* **1994**, *66*, 6. Shibayama, N.; Saigo, S. *J. Mol. Biol.* **1995**, *251*, 203–209. Shen, C.; Kostic, N. M. *J. Am. Chem. Soc.* **1997**, *119*, 1304–1312.

(35) Crowe, L. M.; Reid, D. S.; Crowe, J. H. *Biophys. J.* **1996**, *71*, 2087–2093.

(36) Chen, C.; Perez-Gonzalez-de-Apodaca, J.; Shannon, C. F.; Khan, I.; Peterson, E. S.; Das, T. K.; Rousseau, D. L.; Friedman, J. M. *Biochemistry* Submitted for publication.